

Figure 1. Distribution of the 7^+ transition strength from the $^{62}\text{Ni}(d,\alpha)^{60}\text{Co}$ reaction.

states between 1.5 and 4.8 MeV with the centroid at 3.9 MeV. This situation is in contrast to what is observed^{1,2} in the $^{58}\text{Ni}(d,\alpha)^{56}\text{Co}$ reaction, where the dominant 7^+ transition strength is to a single state at 2.28 MeV, although there are several much smaller fragments.

- 1) H. Nann, A.D. Bacher, W.W. Jacobs, W.P. Jones, and E.J. Stephenson, Phys. Rev. C 24, 1984 (1981).
- 2) H. Nann, W.W. Jacobs, A.D. Bacher, G. Cravens, W.P. Jones, and E.J. Stephenson, Phys. Lett. 109B, 175 (1982).

DWBA INADEQUACIES SAMPLED IN THE ANALYSIS OF THE $^{60}\text{Ni}(p,d)^{59}\text{Ni}$ REACTION AT 94 MeV BOMBARDING ENERGY

H. Nann, D.W. Miller, W.W. Jacobs, D.W. Devins, and W.P. Jones
Indiana University Cyclotron Facility, Bloomington, Indiana 47405

DWBA calculations for the analysis of the angular distributions of the differential cross section and analyzing power, measured in the $^{60}\text{Ni}(p,d)^{59}\text{Ni}$ reaction at 94 MeV, were performed with the computer code DWUCK4. The proton parameters were derived from the work of Schwandt et al.¹, whereas several deuteron potentials were used. The first deuteron potential parameter set, D_1 , was taken from Duhamel et al.², the second set, D_2 , from the global fit of Daehnick et al.³ and the third set, D_3 , from Stephenson et al.⁴, who enlarged and refitted the 80 MeV- ^{58}Ni data base of Daehnick et al.³ The bound-state wave functions were calculated in a Woods-Saxon well with $r_n=1.25$ fm and $a_n=0.75$ fm and a Thomas spin-orbit term with the usual $\lambda=25$ factor. The well depth was adjusted to yield the neutron separation energy.

The influence of the different deuteron parameter sets on the calculated differential cross section and analyzing-power angular distributions was studied for the $2p_{1/2}$, $2p_{3/2}$, $1f_{5/2}$ and $1f_{7/2}$ transitions to the

states at 0.46, 0.00, 1.68 and 1.95 MeV, respectively. As a first step, standard zero-range (ZR) calculations were performed. The results are shown in the top portion of Figs. 1 and 2. The calculations account for the gross features of the differential cross sections (see Fig. 1) but fail completely to reproduce the experimental patterns of the analyzing powers (see Fig. 2). Although the three deuteron potential sets predict no marked differences in the shapes of the differential cross section angular distributions, there are up to 40% differences in the calculated magnitudes of the cross section, which depend on the potential set and the orbital from which the neutron is picked up (see, for example, the $2p_{1/2}$ versus $1f_{7/2}$ transfer). The shapes of $A_y(\theta)$ predicted by the three sets of deuteron potentials are quite different from each other and resemble by no means the experimental patterns. For example, in the case of the $2p_{1/2}$ and $2p_{3/2}$ pickup, large positive analyzing powers were measured for angles greater than 15° , whereas the calculations

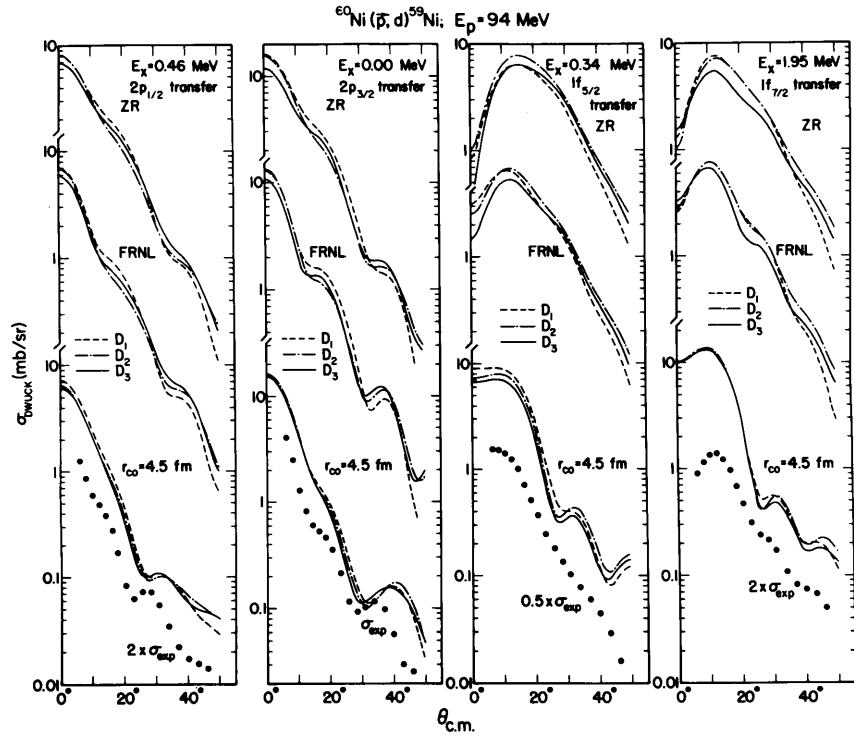


Figure 1. DWBA results for the differential cross sections using three different deuteron optical parameter sets.

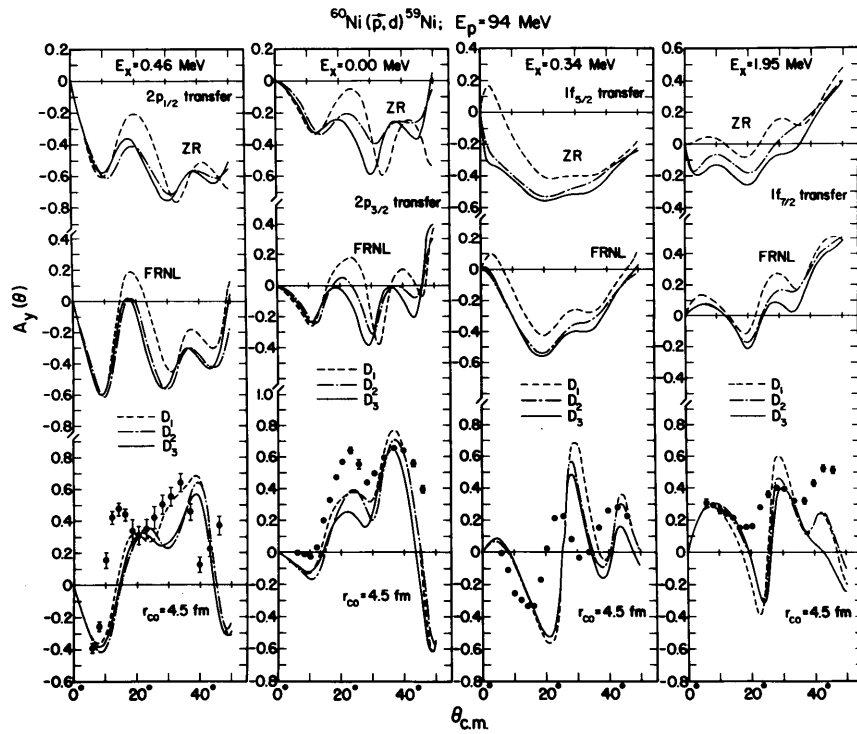


Figure 2. DWBA results for the analyzing power using three different deuteron optical parameter sets.

predict large negative values. In a second step, finite range and nonlocality corrections were included in the DWUCK4 calculations. The values used for the nonlocality parameters were 0.85 fm for the proton and the neutron and 0.54 fm for the deuteron. The finite range parameter was set to 0.621 fm. The results (labeled FRNL) are shown in the middle portion of Figs. 1 and 2. The shape changes for the differential cross sections and analyzing powers are small, although some improvement to account for the experimental features is noticeable. Since these finite range and nonlocality corrections dampen the form factor in the nuclear interior, this effect was further investigated by introducing a lower radial cutoff which artificially localizes the reaction to the nuclear surface. The results for a lower cutoff radius of $r_{co}=4.5$ fm are shown in the bottom portion of Figs. 1 and 2. A vastly improved agreement with the experimental analyzing power angular distributions was obtained, whereas the shapes of the differential cross sections remained essentially unchanged. This suggests quite strongly that the reaction is localized at the nuclear surface and that the present DWBA calculations do not suppress the nuclear interior correctly. This is corroborated by the experimental observation of a j -dependence in the differential cross section angular distributions, an effect already discussed quite some time ago by Ohnuma and Yntema.⁵

All these different inputs into the DWBA calculations yield different magnitudes of the differential cross sections. Unfortunately, the calculated magnitudes depend quite strongly on the orbital from which the neutron is picked up. This fact does not allow a reliable extraction of relative spectroscopic factors for the pickup from different orbitals. Only relative spectroscopic factors for the

pickup from one particular orbital can be determined with some confidence, since all potential sets and adjustments of the parameters yield the same Q -value dependence of the differential cross section within 10%.

Another uncertainty in the DWBA calculations, which influences the magnitude of the differential cross section, is the choice of the geometrical parameters of the Woods-Saxon well in which the picked-up neutron is bound. This sensitivity was investigated again for the $2p_{1/2}$ (0.46 MeV), $2p_{3/2}$ (0.88 MeV), $1f_{5/2}$ (1.68 MeV) and $1f_{7/2}$ (1.95 MeV) transitions. The deuteron optical parameter set D_2 was used together with the above-mentioned finite range and nonlocality corrections. The results for the most frequently used geometrical parameters of $r_0=1.25$ fm for the radius and $a=0.65$ fm for the diffuseness are shown as solid lines in Fig. 3. As a next step, the diffuseness was increased to $a_n=0.75$ fm. The results, shown as dashed dotted lines in Fig. 3, yield very few changes of the magnitude of the differential cross section for the $\lambda_n=1$ transitions and somewhat larger changes for the $\lambda_n=3$ transitions.

A decrease in the radius to $r_n=1.17$ fm, a value which corresponds to the rms radius of a $1f_{7/2}$ neutron in ^{49}Ti as determined by large angle electron scattering,⁶ resulted in much larger changes in the magnitude of the differential cross sections, especially for the $\lambda_n=3$ transitions (dashed curves in Fig. 3). In summary, none of these variations of the geometrical parameters for calculating the bound state wave function yields any dramatic changes in the shapes of the differential cross section and analyzing power angular distributions, but introduces a large dispersion of the magnitudes of the differential cross section which depends quite strongly on the orbital

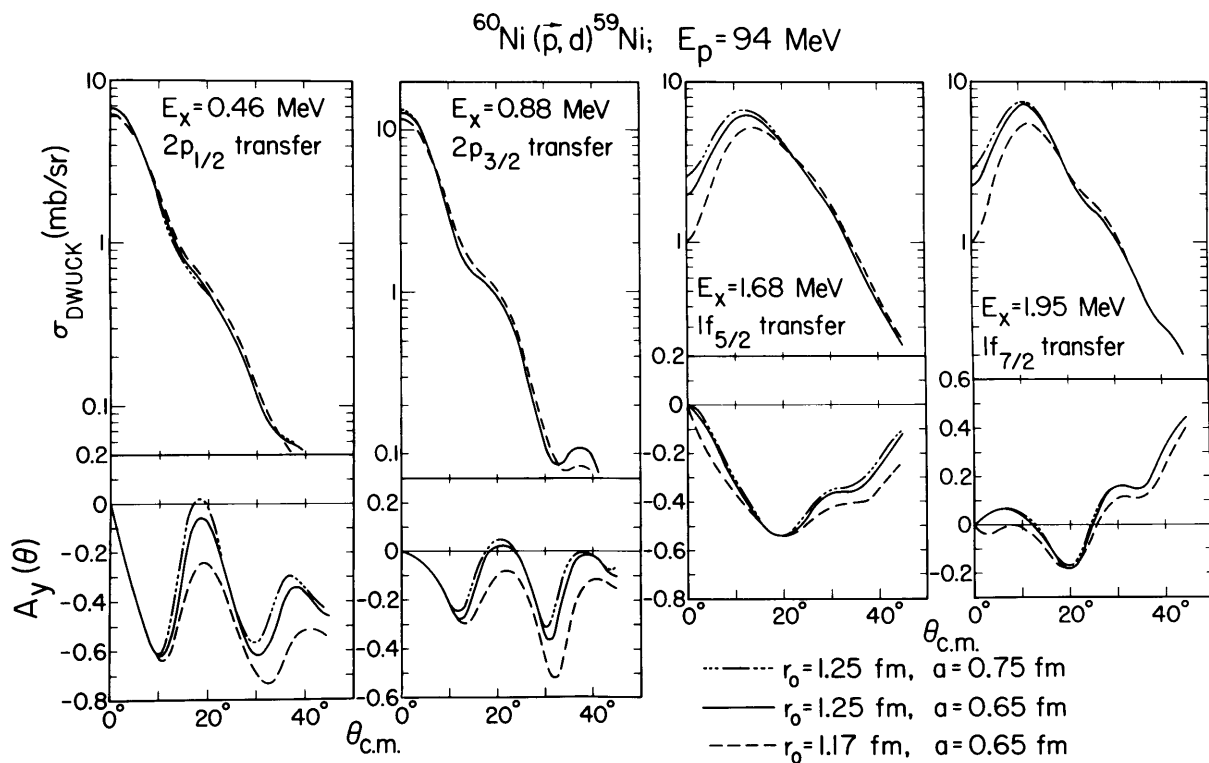


Figure 3. DWBA results for different geometrical parameters of the bound-state well.

from which the neutron is picked up. It has been recently suggested⁷ that this uncertainty in the geometrical bound state parameters can be reduced considerably by using information on valence-nucleon wave functions from electron scattering experiments.

- 1) P. Schwandt et al., Phys. Rev. C 26, 55 (1982).
- 2) G. Duhamel, L. Marcus, H. Langevin-Joliot, J.P. Didelez, P. Narboni, and C. Stephan, Nucl. Phys. A174, 485 (1971).

- 3) W.W. Daehnick, J.D. Childs, and Z. Vrcelj, Phys. Rev. C 21, 2253 (1980).
- 4) E.J. Stephenson et al., Phys. Rev. C, in press.
- 5) H. Ohnuma and J.L. Yntema, Phys. Rev. 178, 1654 (1969).
- 6) S.K. Platchkov et al., Phys. Rev. C 25, 2318 (1982).
- 7) A.E.L. Dieperink and I. Sick, Phys. Lett. 109B, 1 (1982).